Journal of Visualization, Vol. 12, No. 2 (2009) 139-156

Regular Paper

Propagation of Orifice- and Nozzle-Generated Vortex Rings in Air

Syed, A. H.* and Sung, H. J.*

* Department of Mechanical Engineering, KAIST, 373-1 Guseong-dong, Yuseong-gu, Daejeon,305-701, Korea.
E-mail: hjsung@kaist.ac.kr.

Received 8 May 2008
Revised 18 October 2008

Abstract : The effect of the exit geometry of a vortex ring generator was studied experimentally. Two types of exit geometries were chosen: an orifice and a nozzle. Vortex rings were generated by pushing a solenoid-valve-controlled, pressurized-air jet through the circular opening of the orifice or nozzle. Experiments were performed over a wide range of initial Reynolds number ($450 \leq \mathrm{Re} \leq 4580$) and length-to-diameter ratio ($0.7 \leq L/D \leq 7.0$) of the air jet. The exit geometry was found to significantly influence the entire course of propagation of the vortex ring. The orifice-generated vortex ring had superior characteristics to that produced by the nozzle under the same conditions. The vorticity generated along the wall in the orifice exit plane had a negligible effect on the circulation of the vortex ring within the specified range of Reynolds number. Compared to the nozzle-generated vortex ring, the orifice-generated ring showed reduced initial vorticity losses and less diffusive entrainment of ambient fluid. The vortex rings produced by the orifice attained more circulation, less entrainment of ambient fluid and hence rapidly propagated through longer distances in comparison to the nozzle-generated rings.

Keywords : vortex ring, evolution, propagation, pinch-off, mass entrainment.

1. Introduction

A vortex ring is a region of rotating fluid bounded by a closed loop of vortex lines such that the flow pattern takes on a toroidal shape. Vortex rings form due to the rolling of the separated boundary layer around an edge when a jet of fluid impulsively leaves an opening, which is usually circular. For an orifice, the opening is a hole in a plane vertical wall; whereas for a nozzle, it is a cylindrical tube perpendicularly projected out from a vertical wall. The mass of a vortex ring is acquired by convective entrainment from the initial jet and diffusive entrainment from the ambient fluid. The circulation of a vortex ring, which is the source of the ring's propagation, is derived from the initial jet. The velocity, propagation distance and diffusion of a vortex ring are greatly affected by its circulation and ambient fluid entrainment. Knowledge of these parameters is of the utmost importance for understanding the role of vortex ring phenomena in nature as well as its industrial and defense applications.

Previous studies on the influence of orifice and nozzle characteristics on the behavior of a vortex ring are relatively scarce. On the basis of smoke visualizations, Irdmusa and Garris (1987) reported that an orifice vortex ring moves faster and entrains less fluid than a sharp-edged nozzle vortex ring. They attributed the different behaviors observed in these systems to increased detachment of opposite-sense vorticity due to the orifice wall. However, Irdmusa and Garris did not specify the geometrical dimensions of the orifice and nozzle (referred to by Irdmusa and Garris as a

'chimney') and the conditions for the initial jet. In reference to this work by Irdmusa and Garris (1987), Auerbach (1989) commented that the observations of faster motion and less entrainment of fluid in case of the orifice compared to the nozzle are not primarily due to the detachment of an opposite-sense vorticity from the orifice wall. Maxworthy (1977) reported the existence of an opposite-sense vorticity at nozzle exits, and Didden (1979) showed that this opposite-sense vorticity is responsible for reducing circulation of the vortex ring. In a numerical study of vortex rings, James and Madnia (1996) indicated that the circulation of a vortex ring is approximately the same with or without a vertical wall in the exit plane. Using a similarity analysis and flow visualizations for piston-cylinder generated vortex rings in water, Pullin (1979) found differences in the core structure, circulation and diameter of the vortex rings generated at orifice and nozzle openings. In addition to this, in a visualization study of vortex rings generated by a piston-cylinder arrangement in water, Auerbach (1991) found more pronounced effects of Reynolds number on the orifice-generated vortex rings than on the nozzle-generated ones. He further reported 40% ambient fluid entrainment for the system with a nozzle compared to 17% for the orifice system. Although Auerbach (1991) could not determine the reason for the difference in fluid entrainment between the nozzle and orifice, he suggested that the difference has more to do with the form of the streaklines rather than to the opposite-sense vorticity and length of the streaklines. Baird et al. (1977) estimated the mass entrainment fraction for an orifice vortex ring to be 25% of the total mass. Dabiri and Gharib (2004) performed a dedicated experimental study to determine the fluid entrainment fraction for a nozzle vortex ring in water. Using a piston-cylinder type vortex ring generator, they calculated the entrainment fraction from PIV (Particle Image Velocimetry) velocity data to be 30% to 40% of the total volume.

Gharib et al. (1998) suggested that there is an upper limit to the maximum circulation that can be attained by a stable vortex ring. If the circulation of the initial jet exceeds this limit, the ring pinches-off from the initial jet, leaving behind the remainder of the vorticity ejected from the vortex ring generator. In the work of Gharib et al. (1998), vortex rings in water were generated by using a piston-cylinder type vortex ring generator with a cylindrical nozzle as the opening. They reported a critical length-to-diameter ratio (L/D) for the initial jet in the range 3.6 - 4.5, above which pinch-off should occur. Allen & Auvity (2002) and Cater et al. (2004) analyzed the generation of a 'piston vortex' in front of the advancing piston of a typical piston-cylinder type vortex ring generator. They showed that a piston vortex is produced as the moving piston scrapes the boundary layer from the inside of the cylinder. The vortex ring circulation is increased by 33.4% when the piston is flushed by the exit of the cylinder, and by 22.8% when the piston stops within the cylinder at a distance from the exit equal to twice the diameter of the cylinder (Cater et al., 2004).

The literature on vortex rings reveals several differences depending on whether vortex rings are generated via an orifice or a nozzle; however, the findings reported previously also contain several contradictions. The reliability of mass entrainment results obtained using visualization techniques is questionable, as the physical extent of the ring may not be correctly determined (Maxworthy, 1972). In addition, the fact that most previous works do not report the exact initial and boundary conditions makes it difficult to draw conclusions based on a comparison of orifice and nozzle systems. The effect of the opposite-sense vorticity generated along the wall of an orifice-type opening on a vortex ring properties is not yet clear; an accurate analysis is required to determine the exact role of the wall in the plane of the orifice exit on the vortex ring circulation and ambient mass entrainment. Moreover, a comparison of ambient fluid entrainment in a vortex ring via an orifice and via a nozzle has only been made on the basis of flow visualization. Further, the maximization of circulation and pinch-off of the vortex ring via an orifice is yet to be explored. Most previous studies examined piston-cylinder type vortex rings generated in water. However, in order to avoid the effect of the 'piston vortex' on vortex ring circulation, studies are required that use a vortex ring generator that does not involve a piston action. Ambient fluid entrained into a vortex ring shares its momentum, which also enhances the diffusion of the vortex ring by diluting the vorticity concentrated in the vortex ring core. The circulation and mass of the vortex ring jointly affect its propagation and stability.

2. Experimental Setup

Figure 1 shows a schematic of the experimental setup employed in this study. The apparatus consists of a large chamber made up of acryl, whose dimensions (5000×600 ×600 mm) are large enough to reduce any effect of the chamber walls on the vortex ring generation and propagation. Seeding ports are provided at suitable locations in the chamber ceiling to achieve uniform seeding throughout the chamber, which is required to probe the velocity field using PIV. Diethylhexyl sebacate smoke (aerosol particles with sizes of nearly 1 μm) is produced by a seeding generator (Lavision Seeder) and is injected into the chamber through the seeding ports. A vortex ring generator, made up of an acryl cylinder, is mounted at the center of one of the end-walls of the chamber. Pressurized air enters the vortex ring generator near its rear end, passes through a honeycomb and then impulsively leaves through an opening in the lid covering the face-end, thereby generating a vortex ring in the acryl chamber. Two different lids with different opening geometries are used in this study. To provide an orifice type exit geometry, the face-end is mounted with a plane lid having a circular hole at its center. This geometry provides a wall in the plane of the exit face. To provide a nozzle type exit geometry, the face-end is mounted with a lid having a cylindrical nozzle fixed at its center. In this case, there is no wall adjacent to the exit face. Both the orifice and the cylindrical nozzle have the same diameter (3 cm). The length-to-diameter ratio of the cylindrical nozzle is about 1.6.

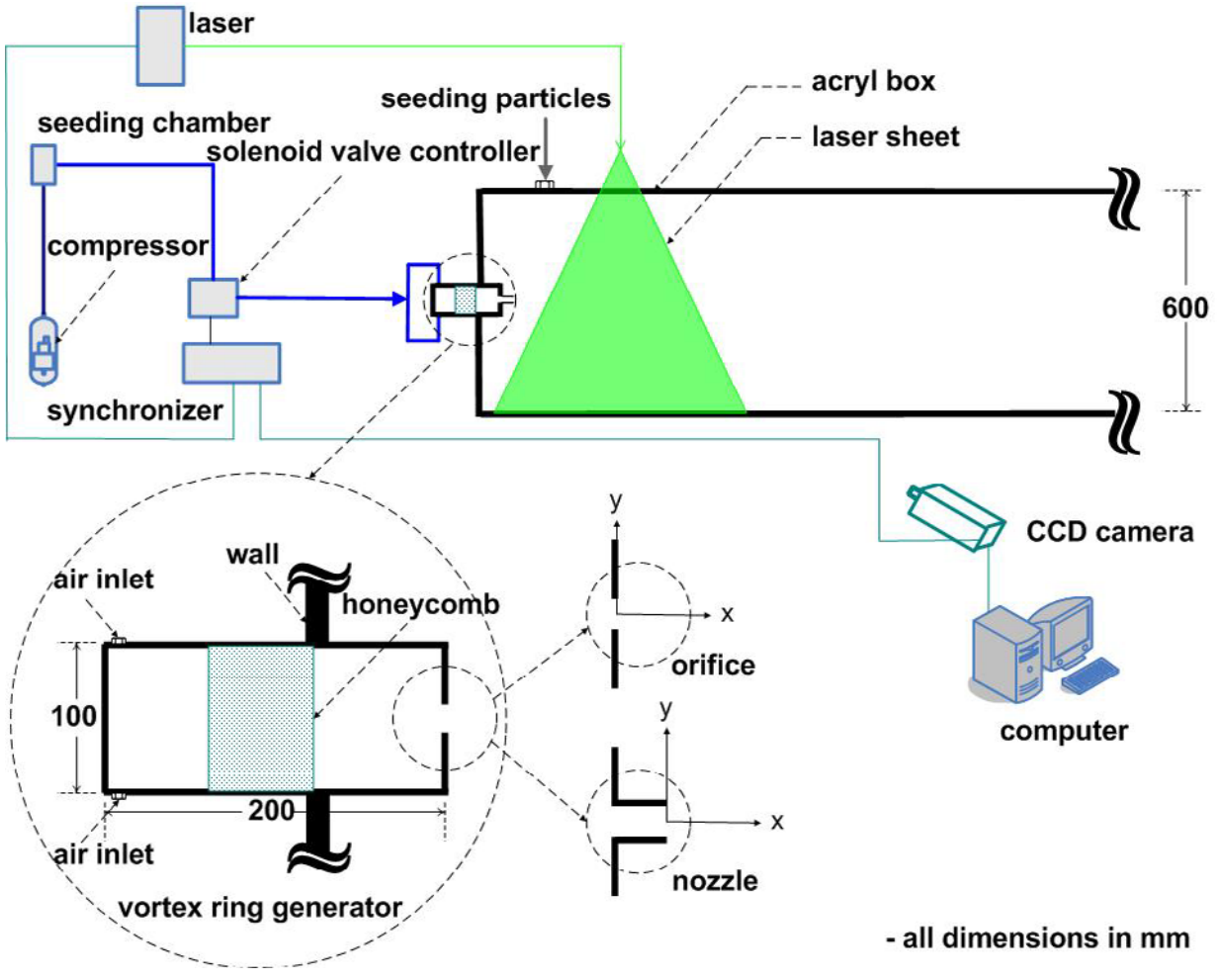

Fig.1 Schematic of the experimental setup and the vortex ring generator.

To generate vortex rings, pressurized air from a dedicated compressor is pushed into the vortex ring generator through a quick-acting solenoid valve. Air-flow through the solenoid valve, and hence the vortex ring generator, is controlled by regulating the air pressure and the valve opening

time. Under the same initial conditions, no measurable difference is found in the exit jet velocity for the orifice and nozzle openings (see Fig.2). This implies that the vortex rings generated by the orifice and the nozzle for the same initial conditions can be compared. For flow visualization, unseeded air from the compressor is directly used to generate vortex rings. Unseeded air is used to obtain a better visualization of vortex rings against the seeded background within the chamber. For PIV measurements, air from the compressor first enters a seeding chamber before entering the vortex ring generator, and the flow is illuminated by a double-pulsed Nd:YAG laser (New Wave Research) with 200 mJ energy per pulse and a pulse width of 6 ns. The time Δt between the consecutive laser pulses is kept at about 3 μs. A PCO SensiCam digital camera with a 1280×1024 pixel CCD array at 30 Hz is employed to capture the PIV field. An 8 channel synchronizer is used to control the timing of the lasers, digital camera and solenoid valve.

With this setup, it is not required to follow a single vortex ring throughout its generation and propagation. Identical vortex rings separated by a time interval of 1 to 4 minutes depending upon the initial conditions are produced with this setup to measure the velocity field. The time interval between consecutive vortex rings avoids any inter-ring interaction and also restores the velocity field inside the chamber to its initial undisturbed state. Thus, each ring can be considered as an isolated vortex ring. Several hundred ring realizations are used in the analysis to minimize random error associated with the sample size.

3. Results and Discussion

In order to compare the orifice- and nozzle-generated vortex rings, it is required to ascertain the same initial conditions for both the orifice and nozzle geometries. Initial jet velocities at the exit of the two geometries have been compared under the identical settings of the pressure-regulator and the solenoid valve. Figure 2 shows a comparison between the instantaneous values of the initial jet

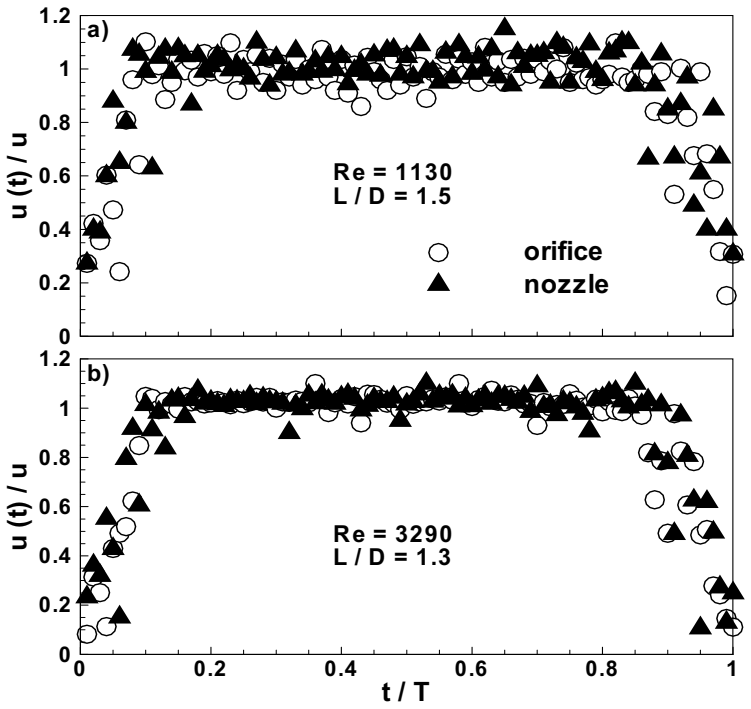

Fig.2 Exit velocity profiles against time. a) Re = 1130, *L/D* = 1.5 and b) Re = 3290, *L/D* = 1.3.

velocities measured at the same axial location with respect to the orifice- and nozzle-openings. Figure 2 shows the initial jet exit velocities under the same initial conditions for the nozzle and orifice geometries for two cases. The initial jet velocities are plotted against the time for one complete

opening and closing valve-cycle for two sets of initial conditions. The time t is normalized by the valve opening time T while the instantaneous velocity $u(t)$ is normalized by u which is the time average of $u(t)$ and is given by $u = \frac{1}{T}\int_0^T u(t)dt$. For a given set of initial conditions, the length L of the initial jet is derived from the instantaneous velocity $u(t)$ and valve-opening time T by $L = \int_0^T u(t)dt$. The initial Reynolds number Re is based on the time-averaged initial jet velocity u and the diameter D of the opening of the vortex ring generator. Figure 2a is for Re = 1130 and L/D = 1.5 (u = 0.55 m/s, T = 0.0825 s) while Fig.2b is for Re = 3290 and L/D = 1.3 (u = 1.6 m/s, T = 0.0237 s). It is observed that the exit jet velocity and its variation with time under a given set of initial conditions for the orifice and nozzle geometries are in good agreement. This ensures that the same initail conditions exist for the orifice- and nozzle-generated vortex rings under a given setting of the pressure regulator and the solenoid valve in the present study. Due to the quick opening and closing action of the solenoid valve, the initial jet velocity programs are reasonably impulsive. The overall velocity variation for one complete valve-cycle is trapezoidal. The normalized velocity $u(t)/u$ is around unity over 85% to 90% of the total time span. The initial jet velocity $u(t)$ reaches around its peak value within the first 5% to 7% of the valve opening time T. Orifice and nozzle generated vortex rings are compared for their evolution and propagation and parametric studies are made for mass entrainment, maximization of circulation, and propagation velocity over a wide range of initial Reynolds number ($450 \leq$ Re ≤ 4580) and length-to-diameter ratio ($0.7 \leq L/D \leq 7.0$) of the initial jet. Table 1 shows a summary of the results included in this paper.

Table 1

phenomenon	Exit boundary	Re	L/D
evolution and propagation	orifice, nozzle	2360	3.6
	orifice, nozzle	3290	4.5
	nozzle	4580	1.2
	nozzle	4580	4.7
mass entrainment	orifice, nozzle	1130	1.5
	orifice, nozzle	1130	3.0
	orifice, nozzle	1660	1.2
	orifice, nozzle	2360	0.9-3.6
	orifice, nozzle	3290	1.1
maximization of circulation	orifice, nozzle	1130	0.9~7.0
	orifice, nozzle	1660	0.9~7.0
	orifice, nozzle	2360	0.9~7.0
propagation velocity	orifice, nozzle	450	1.1
	orifice, nozzle	1130	0.9~8.0
	orifice, nozzle	1660	0.9~8.0
	orifice, nozzle	2360	0.9-7.0
	orifice, nozzle	3290	0.9-6
	orifice, nozzle	4580	2.3

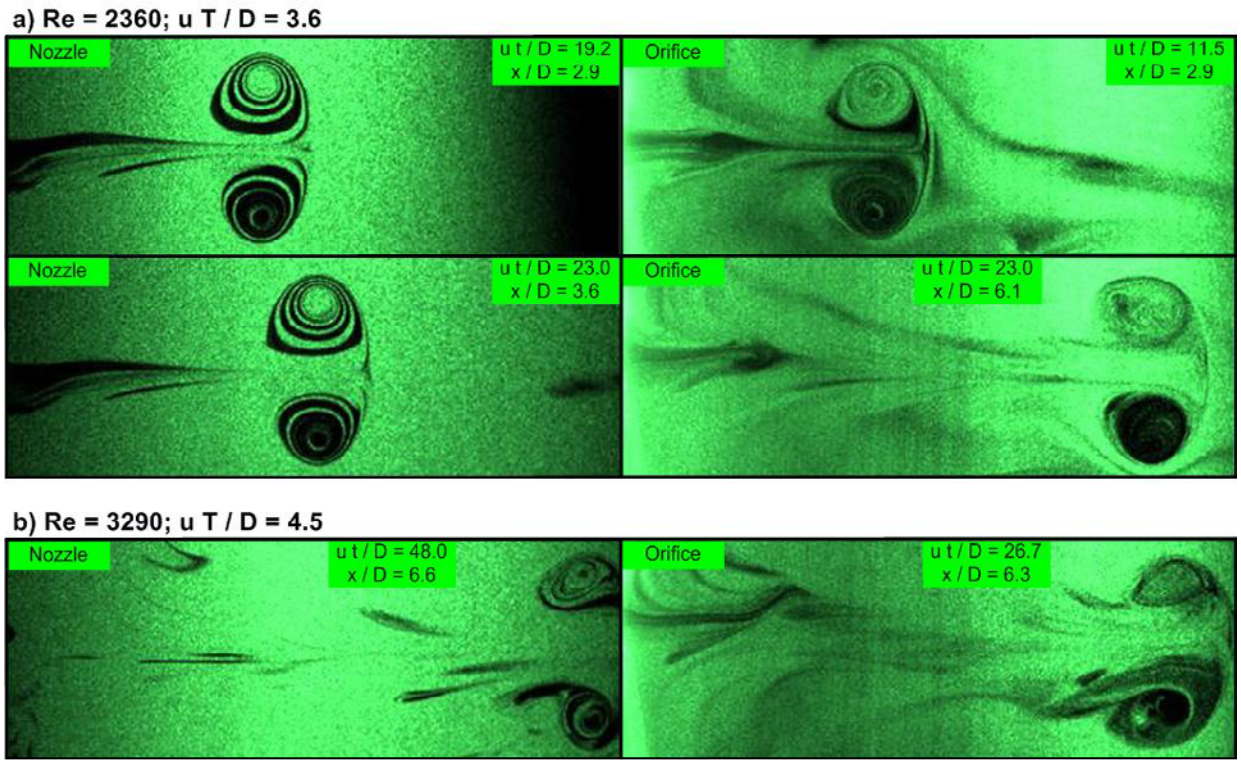

Fig.3 Flow visualizations of nozzle- and orifice-generated vortex rings. a) Comparison of propagation distance and pinch-off. b) Comparison of diffusion pattern.

Figure 3 shows the visualizations of the vortex rings generated under two different Reynolds numbers and length-to-diameter ratios of the initial jet (Re = 2360, L/D = 3.6 and Re= 3290, L/D = 4.5). In the present study, length-to-diameter ratio of the initial jet (L/D) is equivalent to the piston stroke-to-diameter ratio for the typical piston-cylinder type vortex ring generator. In Fig.3a,the vortex ring is just pinching-off from a small trailing jet. The pinch-off occurs when a vortex ring is unable to ingest all the vorticity ejected out of the vortex ring generator. In such a case, the vortex ring cuts itself off from the jet and propagates forward leaving a trailing jet behind it. For L/D = 3.6, the trail is not significant which reasonably agrees with Gharib's observation of pinch-off phenomenon (Gharib et. al., 1998). The small trail behind the ring at L/D = 3.6 may be due to the decelerating velocity observed in Fig.2 near the end of the valve opening-closing cycle. This indicates that there is not a significant difference between the nozzle and orifice geometries regarding the critical value of L/D for the occurrence of pinch-off. This is in agreement with Gharib's observation about the universality of formation number (Gharib et al., 1998). For equal values of the non-dimensional propagation distance (x/D = 2.9), the non-dimensional propagation time ut/D of the vortex ring generated by the nozzle is much different from that of the ring generated by the orifice. Also, pinch-off is about to occur for the same value of x/D (x/D = 2.9) for the vortex rings generated by the nozzle and orifice although the non-dimensional propagation time is different for the two systems. For the same non-dimensional propagation time (ut/D = 23.0), the non-dimensional propagation distance (x/D) for the orifice vortex ring is larger than that for the nozzle. Comparisons of the non-dimensional propagation time and non-dimensional propagation distance between the orifice and nozzle in Fig.3a indicate that the vortex rings generated by the orifice propagate faster than those generated by the nozzle. At non-dimensional time ut/D = 23.0, the vortex ring generated by the orifice has started to diffuse whereas that produced by the nozzle is still retaining its ring shape. The quicker diffusion of the vortex ring generated by the orifice can be attributed to its greater velocity. It also indicates that the diffusion of a vortex ring is more a function of the propagation distance than the propagation time.

Figure 3b shows a visualization of the vortex rings generated by an orifice and a nozzle at

Re = 3290 and *L/D* = 4.5. Although the positions (*x/D*) of the two vortex rings are almost the same relative to the exit of the vortex ring generator, the propagation times (*ut/D*) are different. Both the rings are in their diffusion stages. The behavior observed at this Reynolds number provides further support to the argument that the diffusion of a vortex ring depends more on the propagation distance than the propagation time. A comparison between the orifice-generated vortex ring in Fig.3b with that in Fig.3a at for *x/D* = 6.1 suggests that the diffusion of a vortex ring is more rapid in the system with a higher Reynolds number and a larger *L/D* ratio. In the case of the nozzle-generated vortex ring in Fig.3b, a clear wake is observed behind the diffusing vortex ring. For the orifice system (Fig.3b), however, the wake is not well-defined behind the vortex ring which may be due to the faster propagation of the orifice-generated vortex ring. When a vortex ring propagates forward, viscous dissipation reduces the total pressure of the adjacent fluid. A portion of the diffused vorticity is rejected behind the ring, leading to the formation of a wake because the free stream fluid has sufficient total pressure to convect the rejected vorticity downstream (Maxworthy, 1972). At high initial Reynolds number, however, the rate of viscous dissipation from the fast-moving, orifice-generated vortex ring is large. The total pressure of the adjacent fluid does not remain sufficient to facilitate wake formation and the vorticity is diffused into the surrounding fluid.

Figures 4 and 5 show the results obtained from the simulation of vortex ring phenomenon. Both the results are for an initial Reynolds number Re = 4580 and the impulsive jet leaves through a nozzle geometry. The minimum vorticity cut-off level is 5% of the maximum vorticity level. Figure 4

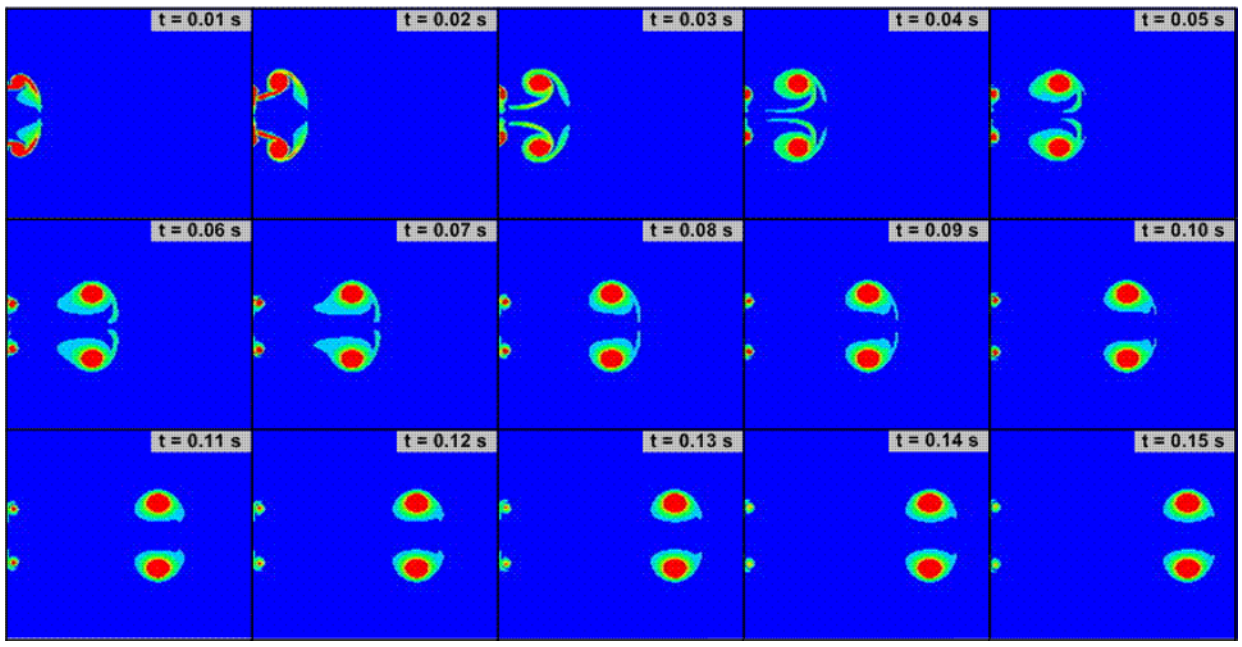

Fig.4 Vorticity field showing the evolution and formation of a nozzle vortex ring at Re = 4580, *L/D* = 1.2.

shows the evolution and formation of a vortex ring with an initial Reynolds number Re = 4580 and *L/D* = 1.2. The initial jet is fully engulfed into the vortex ring within the evolution phase. This is in accordance with Gharib's results (Gharib et al., 1998). There is a critical range of *L/D* ratio (3.6 - 4.5) below which all the vorticity are ejected from the vortex ring generator. As the value of *L/D* in Fig.4 is less than the critical range (*L/D* = 1.2), no trailing jet is observed behind the vortex ring. Detachment of vorticity at nozzle exit is observed in Fig.5 which is in accordance with the observations made by Maxworthy (1977) and Didden (1979). The detached vorticity dilutes as the time passes but still exists, at least to some extent, until the completion of formation phase of the vortex ring. This implies that detachment of vorticity takes place even at small *L/D* values and this vorticity may have a significant value. Figure 5 shows the evolution and formation of a vortex ring at Re = 4580 and *L/D* = 4.7. A trailing jet is clearly observed behind the vortex ring in Fig.5. This is in agreement with Gharib's critical range of *L/D* value (Gharib et al., 1998). As the *L/D* value is greater than the critical

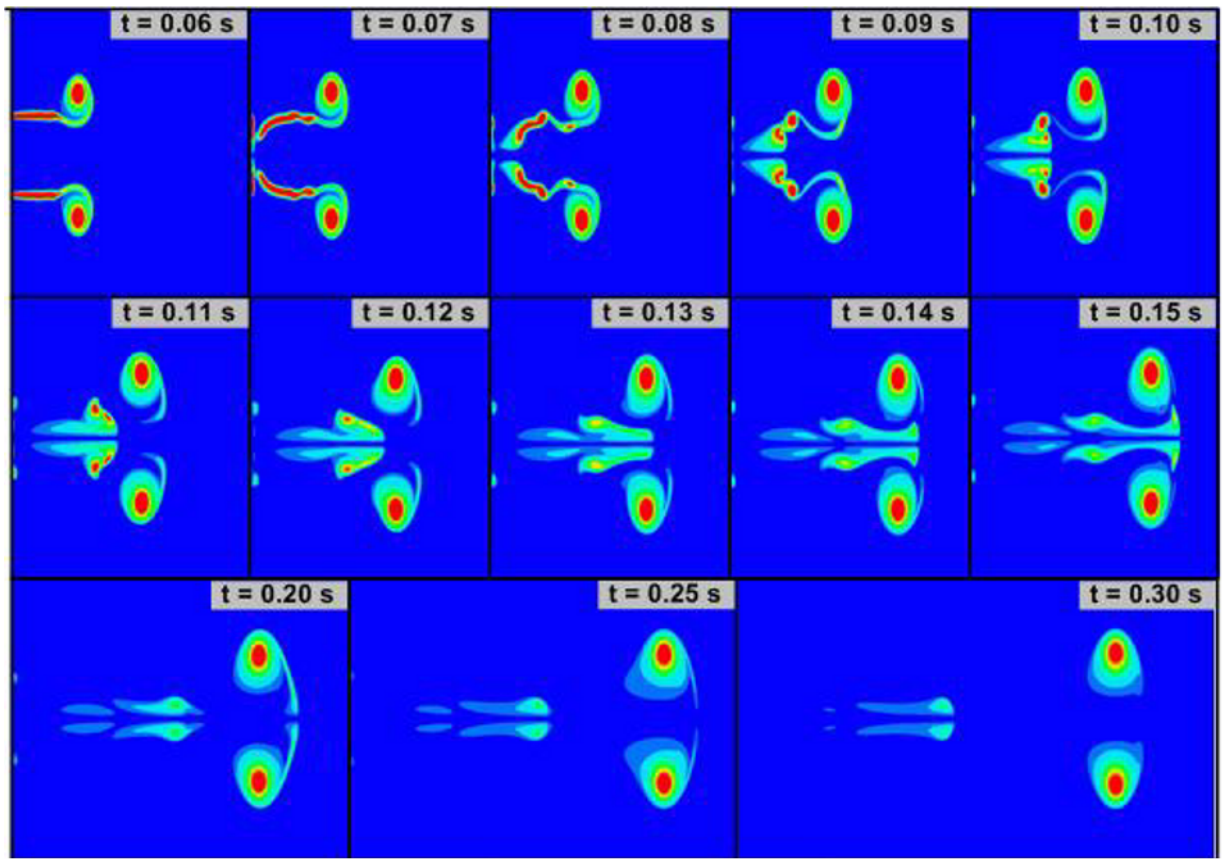

Fig.5 Vorticity field showing the evolution and formation of a nozzle vortex ring at Re = 4580, *L/D* = 4.7.

range, thus all the vorticity of the initial jet could not be ingested into the vortex ring. The vortex ring attained its peak circulation and then pinches off from the trailing jet, leaving behind the rest of the vorticity. The pinch off of the vortex ring begins at t = 0.10 s and the ring starts to separate itself from the initial jet. At about t = 0.13 s the initial jet again catches the vortex ring and as a result a bulge is observed in the vortex ring. This is because the Reynolds number of the initial jet is fairly high. The vortex ring again starts to pinch off from the initial jet after t = 0.15 s and successfully leaves a trailing jet behind it. The vorticity level in the trailing jet is not high because the *L/D* value is marginally greater than the critical range of *L/D* value for the occurrence of pinch off. In contrast with Fig.5, the formation phase of the vortex ring is completed after it successfully pinches off from the vortex ring.

In previous studies, no significant difference was observed between the sizes of the vortex rings generated by an orifice and a nozzle because the physical extent of a vortex ring cannot be accurately determined on the basis of flow visualizations. This problem can be solved by defining a vortex bubble (see Fig.6) in a reference frame that moves with the vortex ring (Dabiri and Gharib, 2004). The PIV velocity field measured in a stationary frame of reference is transformed into the moving frame of the vortex ring. This is accomplished by superimposing a free-stream axial flow with a magnitude equal to the axial velocity of the ring on the PIV field. Streamlines plotted in the resulting velocity field define the physical extent of the vortex ring, which is called the vortex bubble. Comparison of the sizes of nozzle- and orifice-generated vortex bubbles at the same instants (ut/D = 24.3 and 53.7) is shown in Fig.6. The growth of the vortex bubbles generated by the orifice and the nozzle as they move downstream shows that the vortex bubble generated by the nozzle has a greater volume than that produced by the orifice both in the early and late stages. During the initial rolling

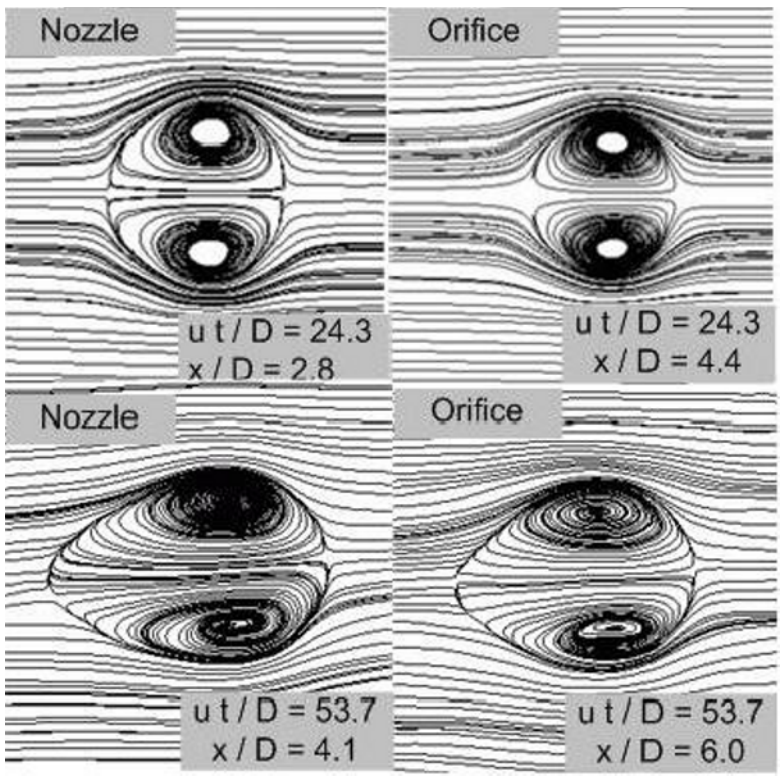

Fig.6 Vortex bubbles for nozzle- and orifice-generated vortex rings with Re = 2360, *L/D* = 0.9

process of vorticity around the exit edge, a greater mass of ambient fluid is entrained into the ring by the nozzle. This is due to the fact that during the evolution of the vortex ring around the edge of the nozzle, the whole periphery of the ring is exposed to the ambient fluid and hence there is a larger surface area through which ambient fluid can ingress. During the evolution of the vortex ring produced by the orifice, by contrast, the ring is shielded from the ambient fluid by the wall in the exit plane of the vortex generator. As the impulse is the same for both the nozzle and orifice systems, the orifice-generated vortex ring propagates faster than the ring produced by the nozzle due to its smaller volume and/or mass. Moreover, in the later stages, the slower propagation of the vortex ring evolved from the nozzle allows more ambient fluid to ingress into the ring per unit propagation distance.

Figure 7 compares the radii of the vortex ring cores for the orifice and nozzle systems at two different Reynolds numbers (Re = 2360 and 4580) and four different length-to-diameter ratios (*L/D*). $r/R - 1$ represents the difference between the radii of the vortex ring and the vortex generator exit, where the radius of the vortex ring core (r) is normalized by the radius (R) of the exit opening of the vortex ring generator. Generally, the nozzle-generated vortex rings have a larger core radius in comparison with the orifice-generated vortex rings. At larger *L/D* (*L/D* = 3.6) for intermediate Reynolds number (Re = 2360), the distance between the two curves of radii is increased. In Fig.7a, the curves start at larger value of non-dimensional time because in the initial stages the radius of the vortex ring core is smaller than the radius of the exit of vortex ring generator. As the Reynolds number is not high (Re = 2360) and *L/D* = 0.9, the radius of vortex ring core is significantly small in the early stages. The difference between the core-radii of orifice- and nozzle-generated vortex rings seems to be more sensitive to *L/D* than to Re. The smaller core-radius of the orifice vortex ring in comparison with the nozzle vortex ring indicates that the growth of the orifice vortex ring is restricted during its evolution. The wall adjacent to the orifice exit restricts the free expansion of the vortex ring during the initial roll-up of the separated boundary layer at the vortex generator exit. This also explains why the difference between the core-radii of the orifice- and the nozzle-generated vortex rings is found to be more sensitive to *L/D* than to Re. The higher *L/D* at a certain Reynolds

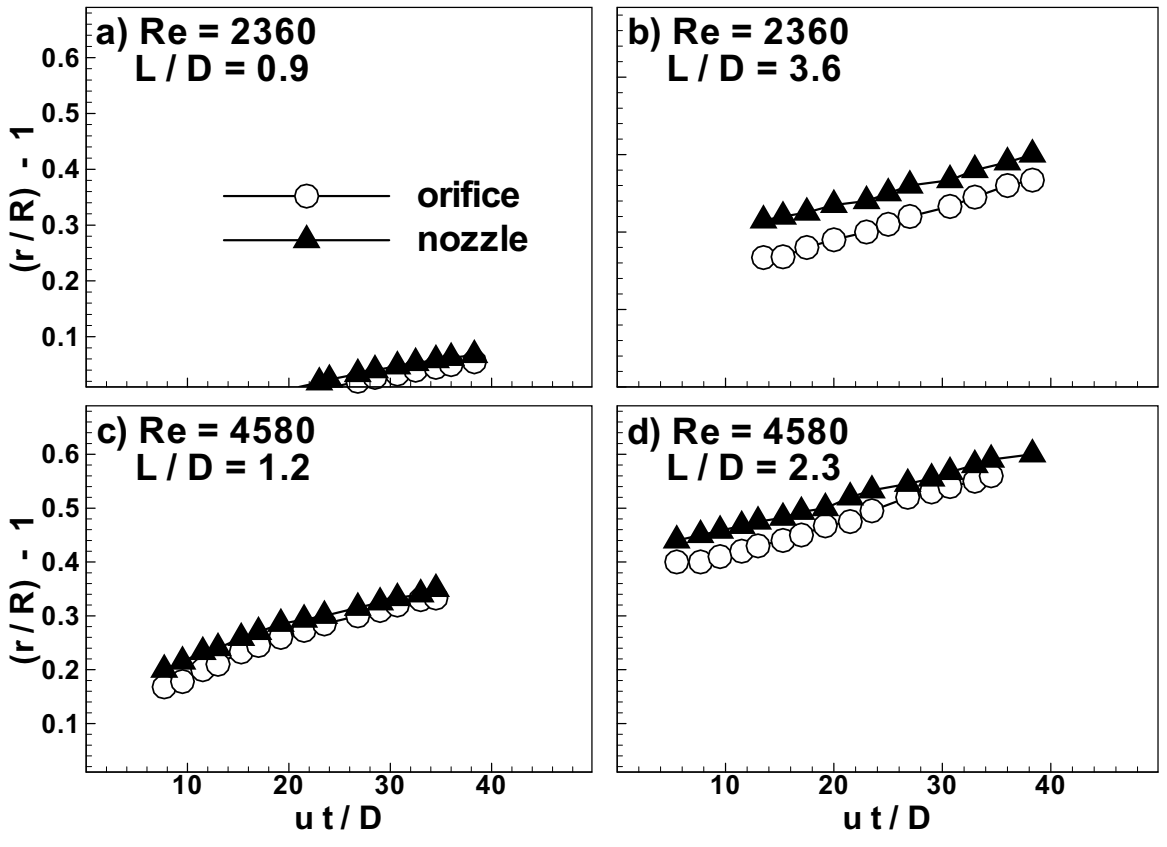

Fig.7 Comparison of core radii of orifice- and nozzle-generated vortex rings.

number means the larger initial mass of the vortex ring with the same initial impulse. Thus, the presence of the orifice wall limits the initial growth of the vortex ring more severely at higher *L/D*. At higher Reynolds numbers the ring is rapidly carried away from the exit of the vortex ring generator which reduces the role of the orifice wall.

Figures 8 to 10 show the mass of ambient fluid entrained into the vortex ring in terms of a fraction of the total mass of the ring. The diffusive mass entrainment fraction of ambient fluid is calculated by the method employed by Dabiri and Gharib (2004). The extent of the vortex bubble is determined by imposing the convective velocity of the vortex ring on the velocity field determined from the PIV data, as discussed previously in relation to Fig.6. In contrast to Dabiri and Gharib (2004), no counter-current was employed in the present work to keep the vortex ring in the measuring window. Rather, identical vortex rings were generated for each PIV measurement using a computer-controlled vortex generator. Phase synchronization was ensured by the use of a centralized digital synchronizer. The volume $V_B(t)$ of a vortex bubble at any instant t is calculated by geometrical considerations. The fluid volume $V_C(t)$ convected into the vortex ring from the vortex ring generator in the same time t is given by,

$$V_C(t) = \frac{\pi D^2}{4} \int_0^t u(t)\,dt \tag{1}$$

The fraction of ambient fluid entrained into the vortex ring by the process of diffusive entrainment is defined as,

$$entrainment\ fraction = 1 - \frac{V_C(t)}{V_B(t)} \tag{2}$$

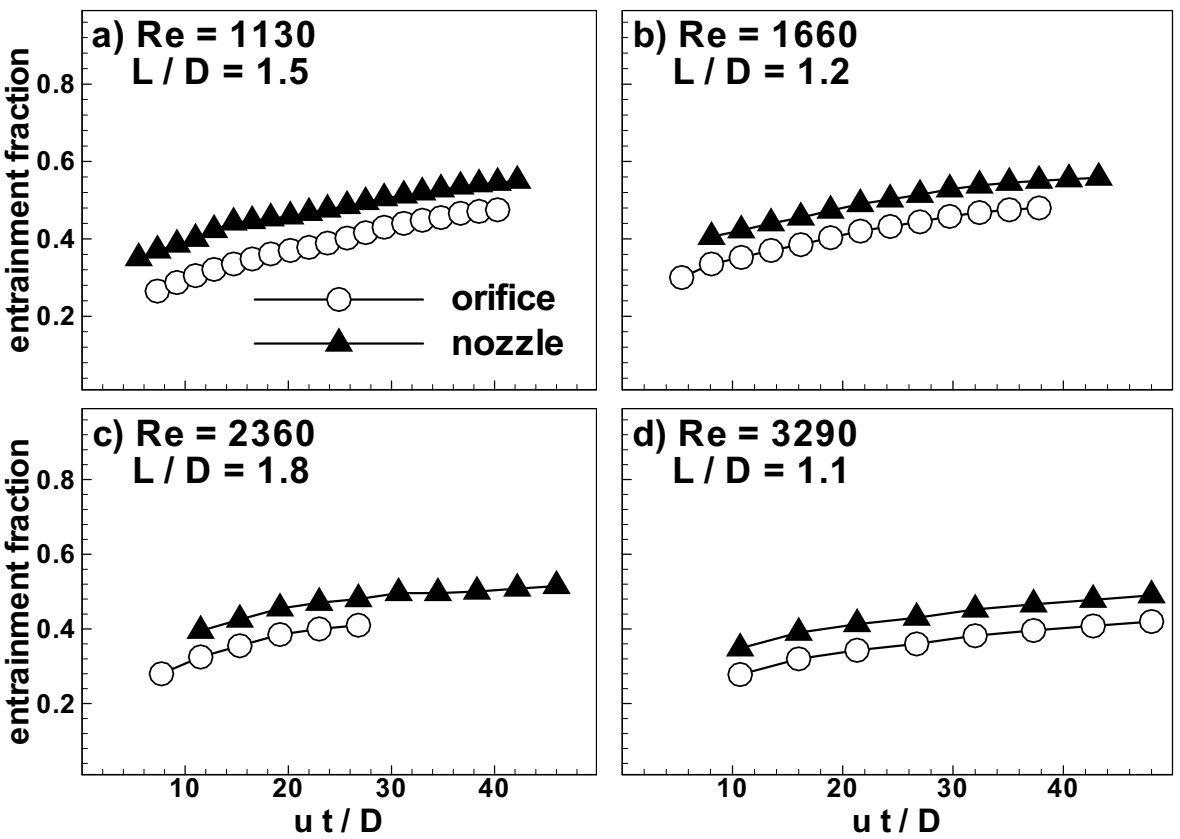

Fig.8 Comparison of ambient fluid entrainment fraction as a function of non-dimensional propagation time for orifice- and nozzle-generated vortex rings.

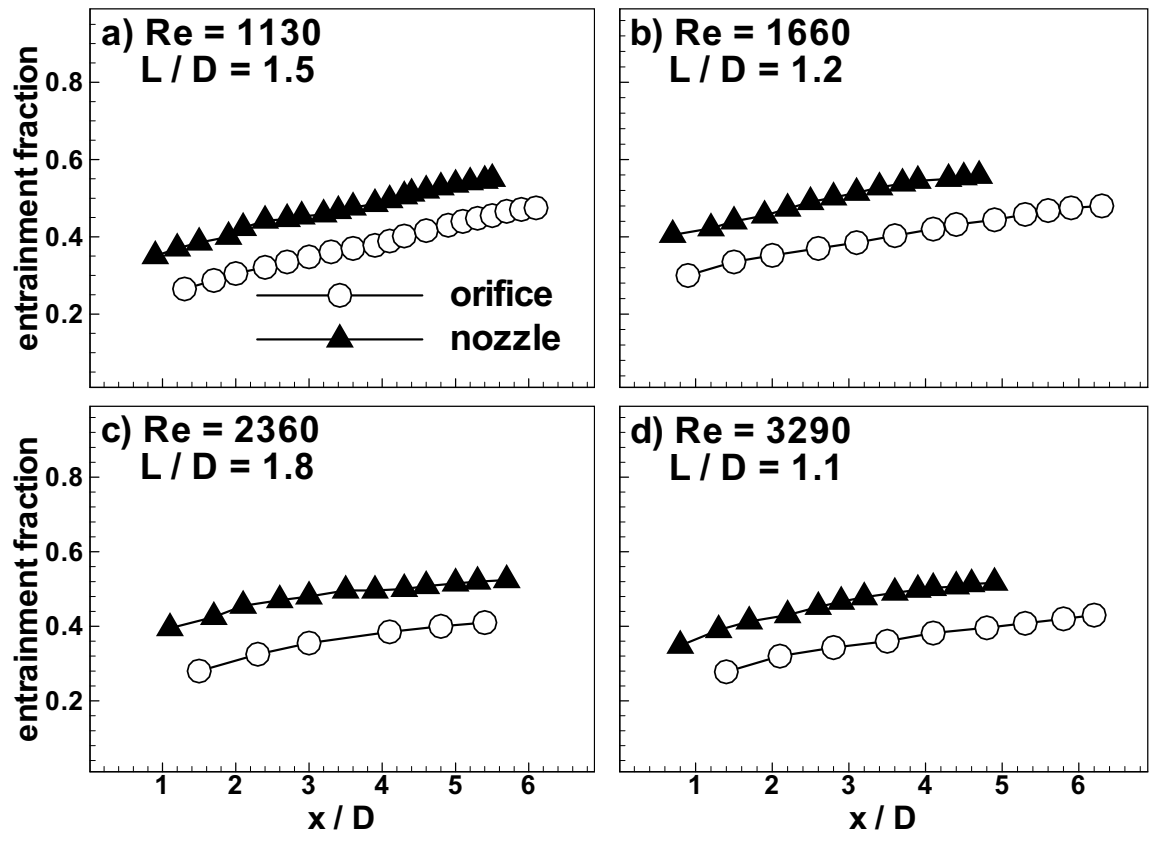

Fig.9 Comparison of ambient fluid entrainment fraction as a function of non-dimensional propagation distance for orifice- and nozzle-generated vortex rings.

In general, the diffusive mass entrainment is between 18% to 60% for both the orifice and nozzle systems (Figs.8 to 10). During the early stage of vortex rings, the entrainment fraction is from 18% to 35%, while in the later stage it increases up to 60% in the data range of the present study. Comparison of ambient fluid entrainment in the orifice and nozzle systems reveals that the entrainment for the nozzle vortex ring is larger than that for the orifice vortex ring and this trend is established right from the initial stages of vortex ring propagation within the range of present study. Irdmusa and Garris (1987) also found a nozzle vortex rings to grow larger than a nozzle vortex ring, however, they did not report a mathematical value. The minimum ambient fluid entrainment fraction for the nozzle system is about 18% whereas it is about 25% for the nozzle system. This reasonably agrees with Auerbach (1991) and Baird et al. (1977). This indicates that the type of vortex ring generator does not have any significant effect on ambient fluid entrainment but the exit geometry does affect the entrainment fraction. The entrainment fraction for the nozzle system is a little less than that of Dabiri and Gharib (2004) who reported 30% to 40%. This may be due to the different initial conditions employed in the present study and also due to the counter-current employed by Dabiri and Gharib (2004) in their study. The presence of the wall in the orifice system restricts the entrainment of ambient fluid. Although ambient fluid entrainment continues as the vortex ring proceeds downstream, most of the entrainment occurs during the initial rolling of the

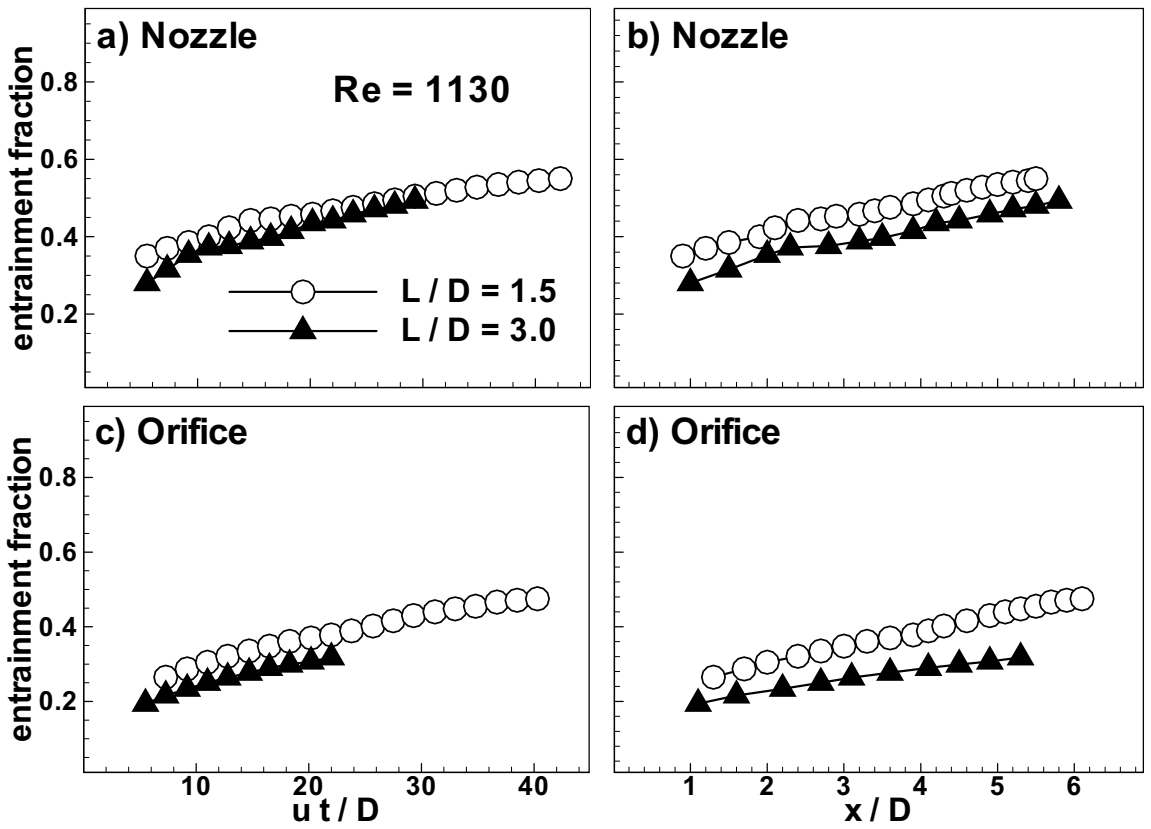

Fig.10 Comparison of ambient fluid entrainment fraction between *L/D* = 1.5 and *L/D* = 3.0 at Re = 1130 for nozzle- and orifice-generated vortex rings.

vortex ring. Due to the further entrainment of ambient fluid, which increases up to 60% within the range of present study, the vorticity of the ring continues to dissipate into the ambient fluid (Maxworthy, 1972) and also spreads over a larger volume of the ring, ultimately leading to the dissipation of the vortex ring. In Figs.8 and 9, the rates of fluid entrainment for the nozzle-generated ring per unit time and per unit propagation distance are greater than those for the orifice-generated ring. Thus, if other conditions remain the same, the vortex ring produced by the orifice should

propagate faster and should be able to propagate through longer distances than that generated by the nozzle (see Fig.14). The difference in the entrainment fractions mainly arises during the initial stage, and then the difference remains almost constant with time as the rings move downstream. This indicates the dependence of the ambient fluid entrainment process on the evolution and formation stages of a vortex ring. In Fig.10, the ambient fluid entrainment fraction slightly decreases for both the nozzle and the orifice as the length-to-diameter ratio of the initial jet increases. The circulation of the vortex ring increases with the length-to-diameter ratio of the initial jet (see Fig.11), and as a result the velocity of the vortex ring increases. Thus, the entrainment of ambient fluid slightly decreases with increasing *L/D* of the initial jet as the ambient fluid gets lesser time to ingress into the vortex ring.

When a vortex ring evolves from an initial jet, it gains circulation from the jet until the circulation attains a maximum value. In this work, the circulation of a vortex ring is calculated by using an in-house developed computer code which calculates the circulation of vortex ring by calculating the loop integral of velocity around the vortex ring boundary making use of the velocity field data obtained by PIV (Arakeri et al., 2004). In this work, the circulation of a vortex ring is calculated by the method employed by Arakeri (Arakeri et al., 2004). Rectangular loops are considered around the boundary of the PIV image of a vortex ring so that they contain all the ring vorticity. An in-house developed computer code calculates the loop integral of velocity making use of the velocity field data obtained by PIV.

$$\Gamma = \oint \vec{U} \cdot d\vec{S} \tag{3}$$

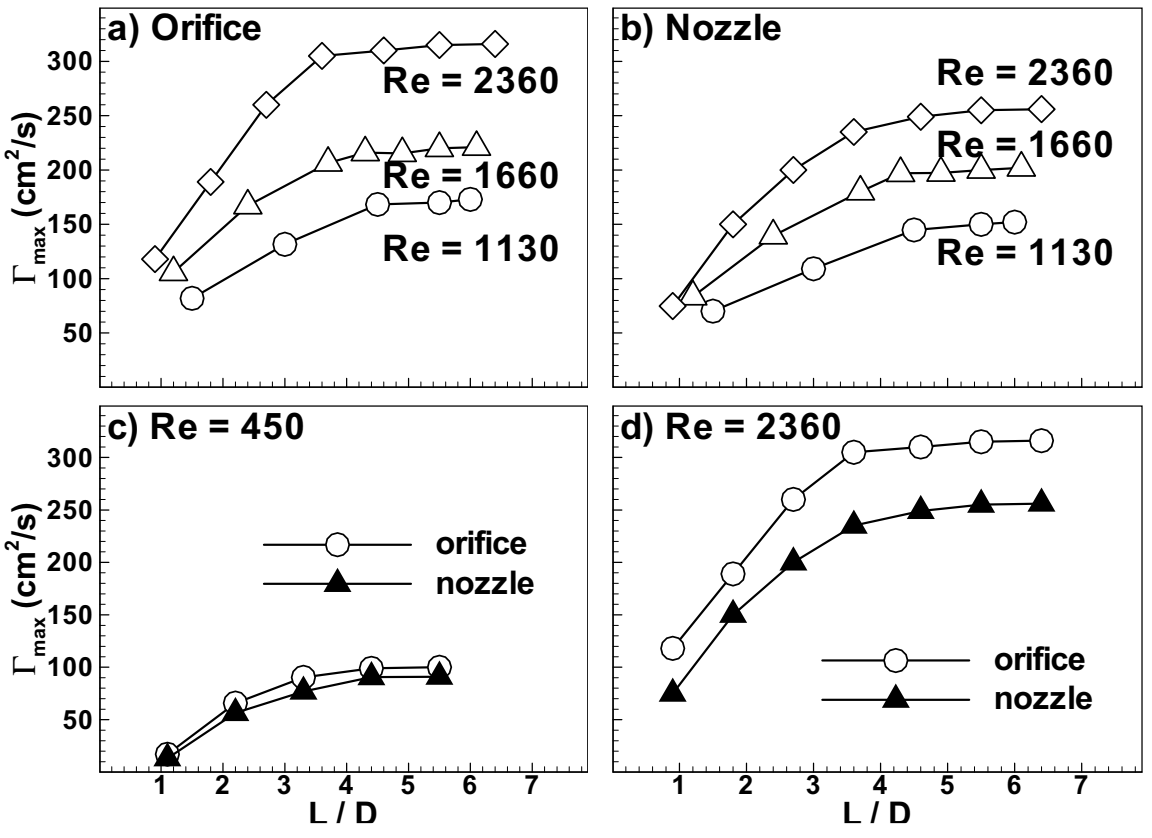

Fig.11 Maximum circulation attained by vortex rings w.r.t. *L/D* ratio a) for orifice-generated vortex rings, b) for nozzle-generated vortex rings, c) comparison between orifice- and nozzle-generated vortex rings at Re = 450, and d) comparison between orifice- and nozzle-generated vortex rings at Re = 2360.

Figure 11 shows the maximum circulation that could be attained by a vortex ring as a function of length-to-diameter ratio of the initial jet. The maximum circulation depends on the

Reynolds number and length-to-diameter ratio of the initial jet, and also on the geometry of the exit of the vortex ring generator. At higher Reynolds number of the initial jet, a vortex ring attains a larger maximum circulation value. The rate of convective fluid entrainment increases with increasing Reynolds number; hence, at high Reynolds numbers, the circulation is engulfed into the ring at a much higher rate than the rate of its rejection and a higher maximum is attained. At any particular Reynolds number, as the length-to-diameter ratio of the initial jet is increased, the maximum circulation also increases. However, there is a limit on the maximum circulation that can be attained by a vortex ring at a particular Reynolds number. If the circulation of the initial jet is greater than this limit, the ring does not take more circulation from the jet and pinches-off (Gharib et al., 1998). Thus, the maximum circulation curves in Fig.11 show asymptotic behavior after a certain *L/D* ratio. The value of this critical length-to-diameter ratio (*L/D*) is, generally, in the range indicated in previous studies on the basis of piston-cylinder type vortex ring generator (Gharib et. al., 1998). This implies that the pinch-off phenomenon and the critical value of *L/D* ratio is not significantly affected by the so called piston-vortex phenomenon which has been reported to occur in piston-cylinder type vortex ring generator (Allen & Auvity, 2002 and Cater et al., 2004). The vortex ring produced by an orifice can attain a larger maximum circulation value than that generated by a nozzle. This difference becomes more pronounced at higher Reynolds number, possibly due to the loss of circulation during evolution of the nozzle-generated ring on account of increased detachment of rolled-up vorticity at the nozzle edge as reported by Maxworthy (1977) and Irdmusa and Garris (1987).

Figures 12 and 13 show the instantaneous circulation of the nozzle- and orifice-generated vortex rings as they advance away from the vortex ring generator. Figure 12 shows the instantaneous circulation with respect to the non-dimensional propagation time for different conditions of the initial jet, while Figure 13 represents the same data as a function of the propagation distance. Instantaneous circulation Γ of the vortex ring is normalized by Γ_s which is the theoretical value of the circulation ejected from the vortex ring generator according to the slug model (Shariff and Leonard, 1992).

$$\Gamma_S = \int_0^t \frac{U^2}{2} dt \tag{4}$$

The instantaneous circulation of the orifice-generated vortex ring exceeds that of the nozzle-generated ring under all conditions. This shows that the effect of opposite-sense vorticity which is supposed to decrease the circulation of an orifice-generated vortex ring is not significant within the range of Re and *L/D* ratio of the present study. As the rate of decay of circulation is, in general, almost the same for both types of vortex ring, the orifice circulation curve remains above the nozzle circulation curve. Again, this difference is established during the initial stages of the vortex ring evolution, indicating that it is due to the adjacent wall in the plane of the orifice. As the surface of the orifice-generated vortex ring is less exposed to the ambient fluid, this ring attains higher circulation due to a lesser loss of vorticity to the ambient fluid on account of viscous diffusion in the initial stages. For the nozzle system, all of the rolled-up vorticity could not be ingested into the ring due to the detachment of rolled up vorticity at the nozzle-edge. This argument is supported by the fact that there is a greater difference between the circulations of the two types of vortex rings at higher Reynolds number. In Figure 13, as the rings proceed downstream, the difference between the instantaneous circulations gradually increases. This effect is due to the fact that a nozzle-generated vortex ring takes a longer time to propagate through the same distance compared to an orifice-generated ring. As a result, there is greater loss of circulation in the nozzle-generated vortex ring due to viscous diffusion and also due to ambient fluid entrainment. It is seen in Figs.12 and 13 that the circulation of the vortex ring is smaller than the total circulation predicted by the slug model even at small *L/D*. It may be due to the over-prediction of the slug model which assumes a uniform velocity profile at the exit of the vortex generator. Another reason is the detachment of rolled-up

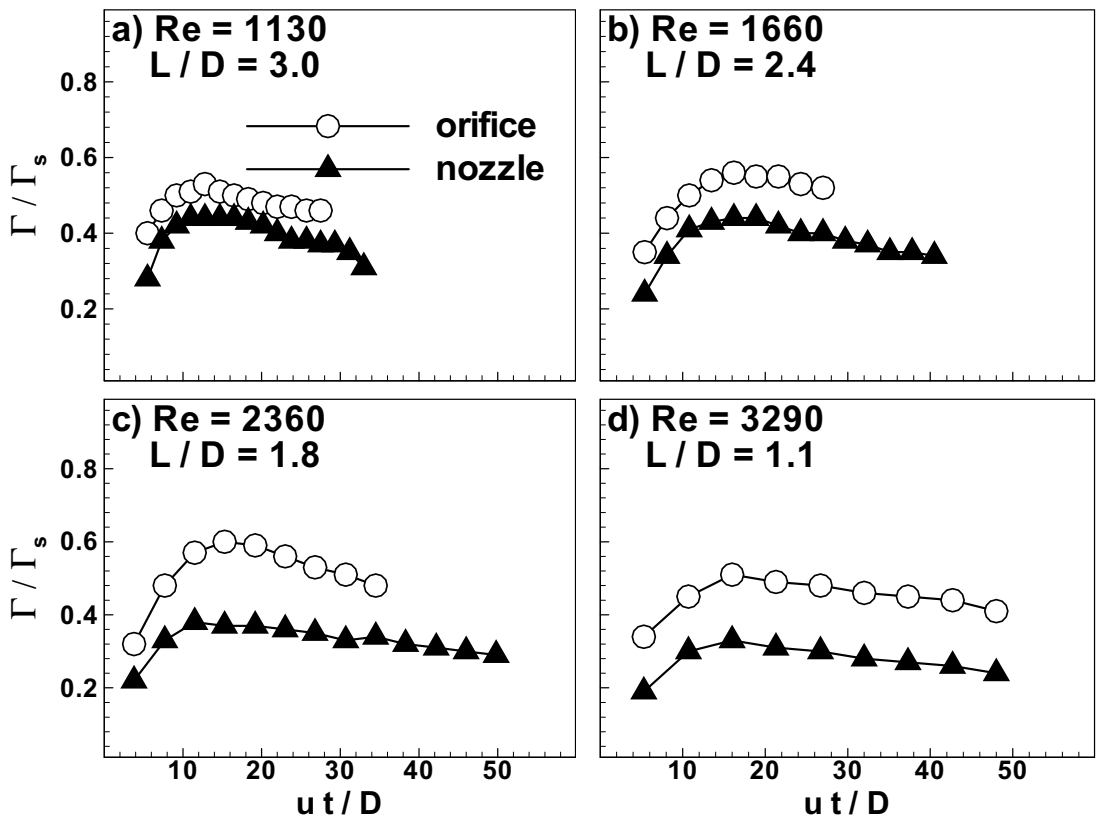

Fig.12 Comparison between the circulation of orifice- and nozzle-generated vortex rings as a function of non-dimensional propagation time.

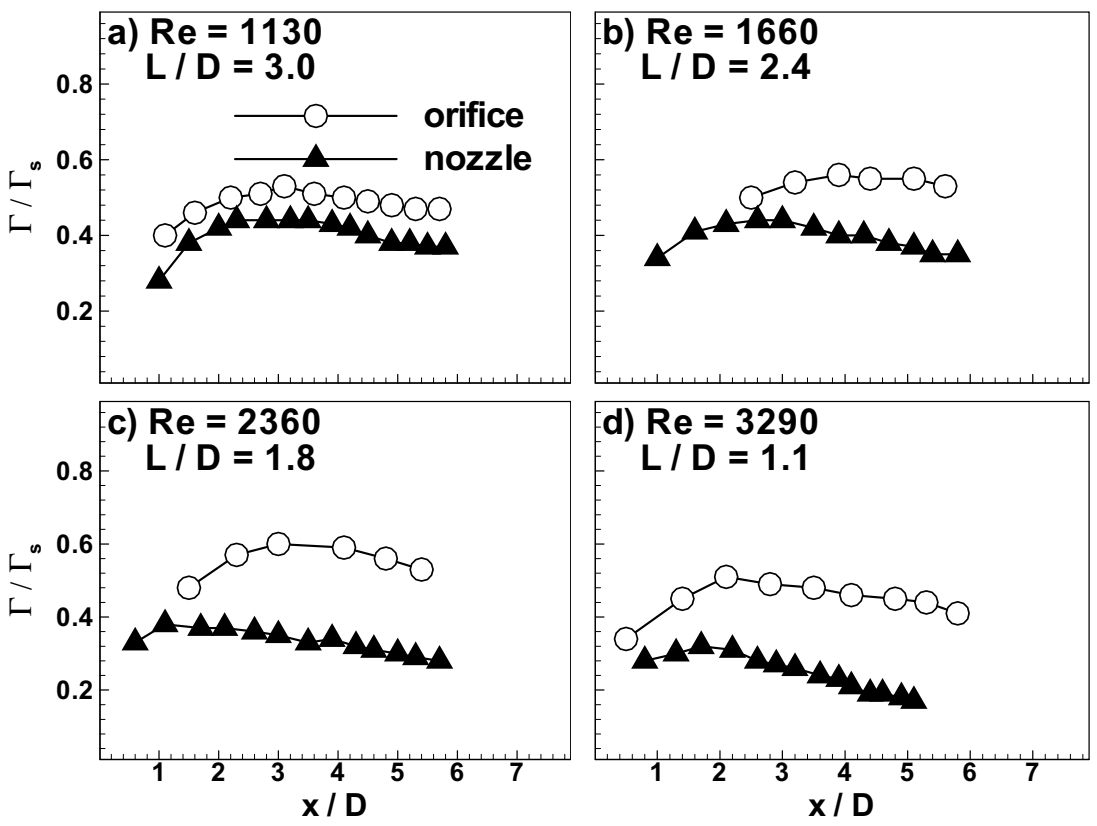

Fig.13 Comparison between the circulation of orifice- and nozzle-generated vortex rings as a function of non-dimensional propagation distance.

vorticity at the vortex generator exit, which increases with increasing the initial Reynolds number. These explain the reason for the decrease in the value of Γ/Γ_s in Figs.12 and 13 when Reynolds number is increased.

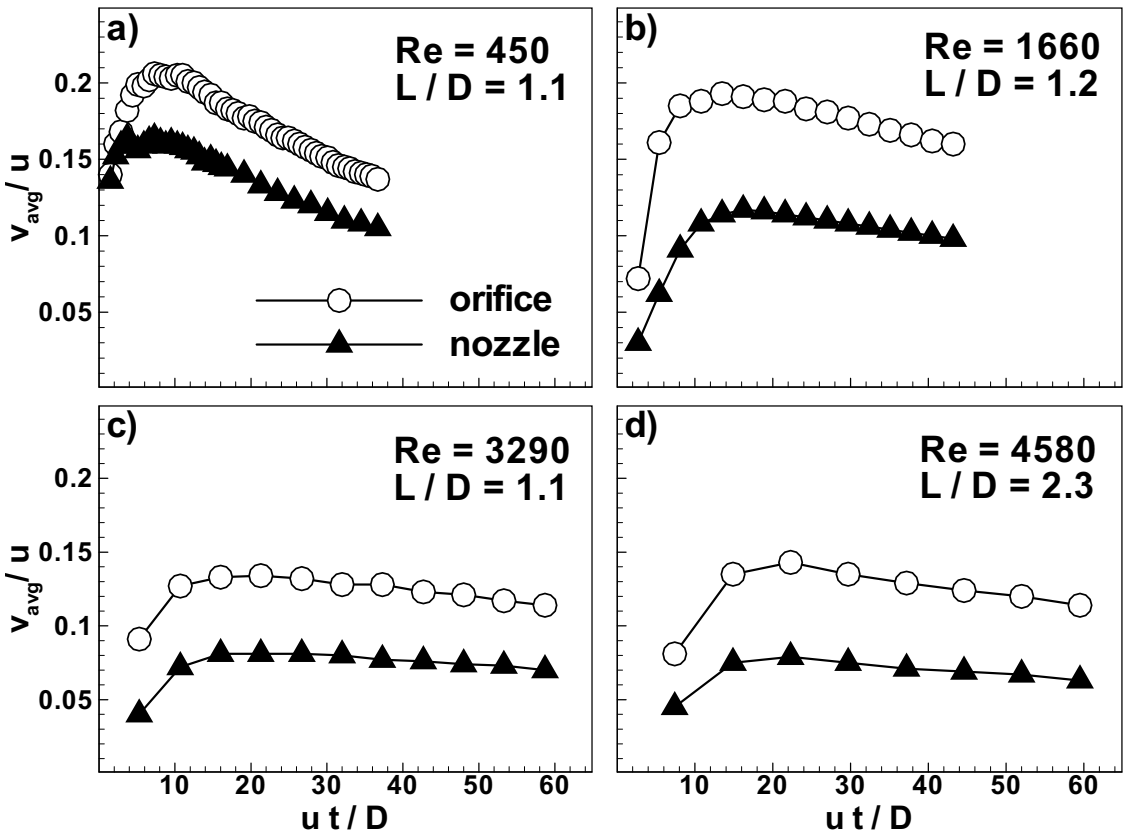

Fig.14 Comparison between the maximum average velocity of orifice- and nozzle-generated vortex rings as a function of non-dimensional propagation time.

Figure 14 shows the average velocity of vortex rings produced under different conditions of Reynolds number and *L/D* ratio. This is in agreement with the quicker propagation of orifice-generated vortex rings in Fig.3. The average velocity is obtained by dividing the propagation distance of a vortex ring from the exit of the vortex generator by the corresponding propagation time. The position of a vortex ring is determined from the location of the vorticity peak in the core of the vortex ring. The average velocity is normalized by the initial jet velocity. The orifice-generated vortex ring shows a larger average velocity than the nozzle-generated vortex ring. At a given distance downstream, the average velocity of the orifice-generated vortex rings is always greater than that of the nozzle-generated rings; this difference increases with increasing *L/D* as well as Reynolds number. Figure 14 compares the variation in the average velocities of the orifice- and nozzle-generated vortex rings as a function of non-dimensional propagation time. Both systems show the same trend. The velocity of a vortex ring is self-induced and is an outcome of circulation of the vortex ring. Hence, it is natural for the average velocity curve to follow the pattern of the circulation curve. Small deviation of the velocity curve from the circulation curve may be attributed to the entrainment of ambient fluid. The entrainment of ambient fluid tends to slow down the vortex ring not only by increasing the mass of the ring but also by the fact that the diffusive mass entrainment phenomenon involves the diffusion of vorticity out from the vortex ring. As expected on the basis of the maximum circulation of the vortex rings (Fig.11), the maximum average velocity in Fig.15 increases with increasing *L/D* and asymptotically approaches a maximum value at higher *L/D* ratios. This maximum value increases

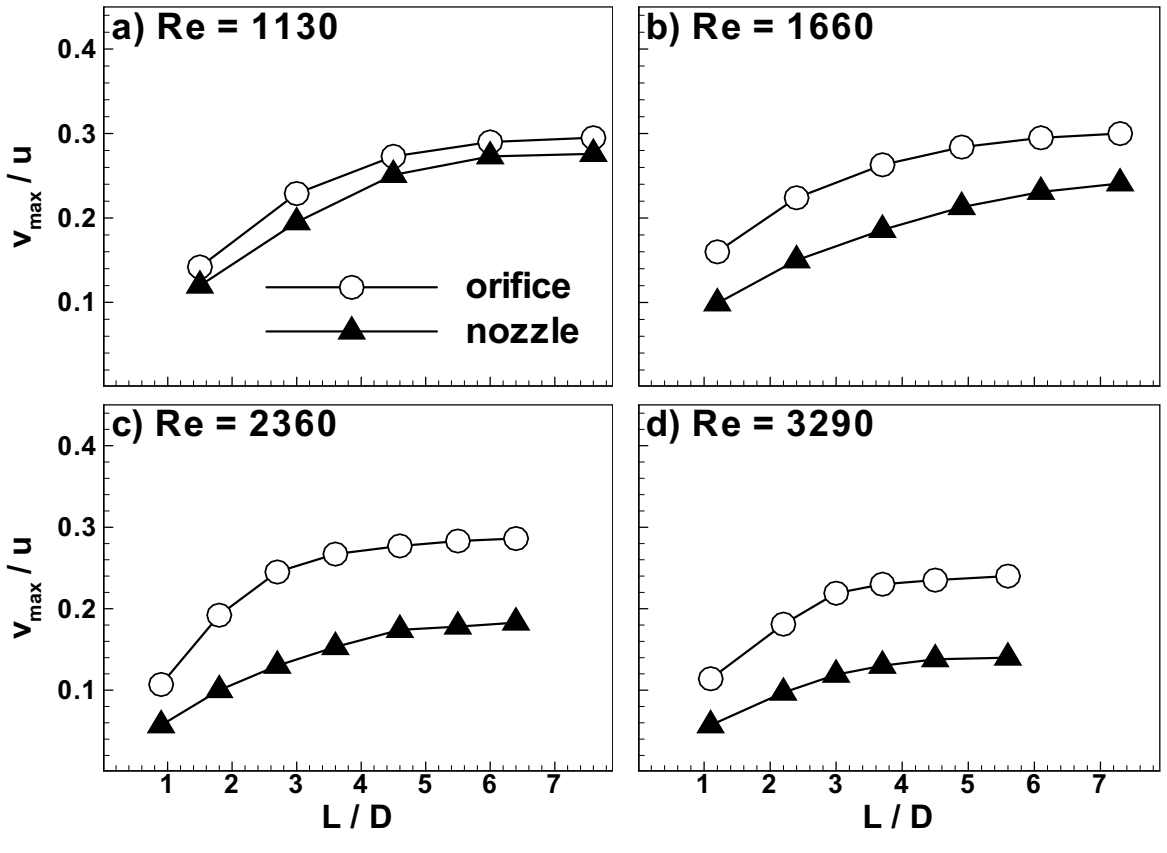

Fig.15 Comparison between the average velocity of orifice- and nozzle-generated vortex rings as a function of non-dimensional propagation time.

with increasing Reynolds number of the initial jet.

4. Conclusions

Vortex rings in air generated by orifice and nozzle geometries have been analyzed and compared. Vortex rings generated by an orifice were found to exhibit superior characteristics to those produced by a nozzle under the same conditions. The effect of the opposite-sense vorticity which is supposed to be generated at the adjacent wall in the exit plane of an orifice was found to be negligible on the circulation of the vortex ring. The presence of the wall adjacent to the orifice not only reduced vorticity detachment at the exit but also reduced the diffusive entrainment of ambient fluid. In the case of the nozzle-type exit geometry of the vortex ring generator, the circulation level of the vortex ring is lower due to larger vorticity detachment near the exit which causes lesser ingestion of rolled-up vorticity into the vortex ring. Moreover, the rolling of the vortex ring around the nozzle edge exposes more surface area to the ambient fluid, resulting in increases in viscous dissipation and diffusive entrainment of ambient fluid. Compared with the nozzle-generated vortex rings, the orifice-generated vortex rings attained more circulation and entrained less ambient fluid, and thus rapidly propagated through longer distances. Due to the superior characteristics of the vortex rings generated by the orifice-type exit geometry, this geometry appears to be a better candidate for industrial applications exploiting the vortex ring phenomenon.

References

Allen, J.J. and Auvity, B., Interaction of a Vortex Ring with a Piston Vortex, J. Fluid Mech. 465 (2002), 353-378.
Arakeri, J.H., Das, D. and Lourenco, L., Vortex Ring Formation at the Open End of a Shock Tube: A Particle Image

Velocimetry Study, Phys. Fluids 16 (2004), 1108-1019.
Auerbach, D., Some Open Questions on the Flow of Circular Vortex Rings, Fluid Dyn. Res. 3 (1988), 209-213.
Auerbach, D., Comment on "Influence of Initial and Boundary Conditions on Vortex Ring Development". AIAA J. 27 (1989), 1145-1146.
Auerbach, D., Stirring Properties of Vortex Rings. Phys. Fluids A 5 (1991), 1351-1355.
Baird, M.H.I., Wairegi, T. and Loo, H.J., Velocity and Momentum of Vortex Rings in Relation to Formation Parameters. Can. J. Chem. Engng. 55 (1977), 19-26.
Cater, J.E., Soria, J. and Lim, T.T., The Interaction of the Piston Vortex with a Piston-Generated Vortex Ring, J. Fluid Mech. 499 (2004), 327-343.
Dabiri, J.O. and Gharib, M., Fluid Entrainment by Isolated Vortex Rings. J. Fluid Mech. 511 (2004), 311-331.
Didden, N., On the Formation of Vortex Rings: Rolling-up and Production of Circulation. J. App. Math. and Phys. (ZAMP) 30 (1979), 101-115.
Gharib M., Rambod, E. and Shariff, K., A Universal Time Scale for Vortex Ring Formation. J. Fluid Mech. 360 (1998), 121-140.
Irdmusa, J.Z. and Garris, C.A., Influence of Initial and Boundary Conditions on Vortex Ring Development. AIAA J. 25 (1987), 371-372.
James, S. and Madnia, C.K., Direct Numerical Simulation of a Laminar Vortex Ring. Phys. Fluids 8 (1996), 2400-2414.
Maxworthy, T., The Structure and Stability of Vortex Rings. J. Fluid Mech. 51 (1972), 15-32.
Maxworthy, T., Some Experimental Studies of Vortex Ring. J. Fluid Mech. 81 (1977), 465-495.
Pullin, D.I., Vortex Ring Formation at Tube and Orifice Openings. Phys. Fluids 22 (1979), 401-403.
Shariff, K. and Leonard, A., Vortex Rings. Annu. Rev. Fluid Mech. 24 (1992), 235-279.

Author Profile

Anwar ul Hasson Syed: He received his B.E. in Mechanical Engineering in 1992 from N.E.D. University, Karachi and M.Sc .(Eng) in Nuclear Power Engineering in 1997 from the same university. After his B.E. and later after his M.Sc. he has been working in a nuclear power plant. His main area of interest was the thermal hydraulics of a nuclear power plant. Presently he is working for his Ph.D. in the department of mechanical engineering in KAIST, Korea. His present research interests are flow control and the operation of a fuel cell in a subzero temperature environment.

Hyung Jin Sung: He received his M.S. degree in Mechanical Engineering in 1980 from KAIST, Korea and his Ph.D. in Mechanical Engineering in 1984 from the same university. He is a professor in the department of Mechanical Engineering, KAIST. He has served as visiting professor in UIUC, Hokkaido University, and UCLA. His current research interests are turbulence and flow control, flow structure interaction, micro/bio fluidics, and fuel cell.